Segregation of Phosphatidic Acid-Rich Domains in Reconstituted Acetylcholine Receptor Membranes†

José A. Poveda, José A. Encinar, Asia M. Fernández, C. Reyes Mateo, José A. Ferragut, and José M. González-Ros*

Centro de Biología Molecular y Celular, Universidad Miguel Hernández, 03206 Elche (Alicante), Spain

Received January 7, 2002; Revised Manuscript Received July 15, 2002

ABSTRACT: Purified Acetylcholine Receptor (AcChR) from *Torpedo* has been reconstituted at low (∼1:3500) and high (∼1:560) protein to phospholipid molar ratios into vesicles containing egg phosphatidylcholine, cholesterol, and different dimyristoyl phospholipids (dimyristoyl phosphatidylcholine, phosphatidylserine, phosphatidylglycerol and phosphatidic acid) as probes to explore the effects of the protein on phospholipid organization by differential scanning calorimetry, infrared, and fluorescence spectroscopy. All the experimental results indicate that the presence of the AcChR protein, even at the lower protein to phospholipid molar ratio, directs lateral phase separation of the monoanionic phosphoryl form of the phosphatidic acid probe, causing the formation of specific phosphatidic acid-rich lipid domains that become segregated from the bulk lipids and whose extent (phosphatidic acid sequestered into the domain, out of the total population in the vesicle) is protein-dependent. Furthermore, fluorescence energy transfer using the protein tryptophan residues as energy donors and the fluorescence probes *trans*-parinaric acid or diphenylhexatriene as acceptors, establishes that the AcChR is included in the domain. Other dimyristoyl phospholipid probes (phosphatidylcholine, phosphatidylserine, phosphatidylglycerol) under identical conditions could not mimic the protein-induced domain formation observed with the phosphatidic acid probe and result in ideal mixing of all lipid components in the reconstituted vesicles. Likewise, in the absence of protein, all the phospholipid probes, including phosphatidic acid, exhibit ideal mixing behavior. Since phosphatidic acid and cholesterol have been implicated in functional modulation of the reconstituted AcChR, it is suggested that such a specific modulatory role could be mediated by domain segregation of the relevant lipid classes.

Ligand-gated ion channels constitute an important family of complex membrane proteins acting as receptors for neurotransmitters (*1*−*3*). The nicotinic acetylcholine receptor (AcChR)[1] from *Torpedo* is a prototypic member of such family and consists of a pentameric transmembrane glycoprotein composed of four different polypeptide subunits (α, *β*, *γ*, and *δ*) in a 2:1:1:1 stoichiometry, positioned around an axis of pseudosymmetry perpendicular to the plane of the membrane (*4*-*6*). Binding of presynaptically released acetylcholine to extracellular sites on the AcChR (*7*) elicits the formation of a transient cation channel (an aqueous pore) within the protein, responsible for the initiation of postsynaptic membrane depolarization. On continuous exposure to the cholinergic agonist, however, the channel opening response becomes blocked and the affinity for the agonist increases, a process known as desensitization (*8*).

In the last two decades and partly due to the abundance of the AcChR in the electric tissue of *Torpedo* and to its cloning during the early eighties, vast studies have appeared on different functional aspects of this and related members of this family of molecules (reviewed in ref *9*). Also, the tridimensional structure of the *Torpedo* AcChR has been determined at 4.6 Å resolution (see ref *10* and references therein). Along these studies, the reconstitution of the purified AcChR protein into artificial liposomes of defined composition have shown that the presence of certain lipids in the reconstituted samples, namely, cholesterol and phosphatidic acid (PA), are important in preserving the ability of the reconstituted AcChR to exhibit an optimal cation channel activity (*11*−*15*). Such effects of lipids on AcChR function are also known to be fully reversible. For instance, McNamee's group used an approach of "re-reconstitution" (reconstituting the protein twice, first in a lipid matrix that does not allow AcChR function, then in whole asolectin lipids) to demonstrate that an "inactive" AcChR regains its function upon a second reconstitution into an appropriate lipid matrix (*13*).

Despite the existing information on the lipid dependence of AcChR function, no satisfactory explanation has been given on the molecular events by which specific lipids exert

† Supported partly by a grant from the DGESIC of Spain (PM1998-0098). J.A.P. is the recipient of a predoctoral fellowship from the "Ministerio de Educación y Ciencia" of Spain.

* To whom correspondence should be addressed. Phone: + 34 96 6658757. Fax: + 34 96 6658758. E-mail: gonzalez.ros@umh.es.

[1] Abbreviations: AcChR, nicotinic acetylcholine receptor; FTIR, Fourier transform infrared spectroscopy; PC, phosphatidylcholine from egg yolk; DMPA, dimyristoyl phosphatidic acid; d-DMPA, perdeuterated Dimyristoyl Phosphatidic acid; DMPC, dimyristoyl phosphatidylcholine; d-DMPC, perdeuterated dimyristoyl phosphatidylcholine; DMPS, Dimyristoyl Phosphatidylserine; DMPG, dimyristoyl phosphatidylglycerol; *t*-PnA, *trans*-parinaric acid; DPH, 1,6-diphenyl-1,3,5-hexatriene; DSC, differential scanning calorimetry; FRET, fluorescence resonance energy transfer.

10.1021/bi0200099 CCC: $22.00 © 2002 American Chemical Society
Published on Web 09/11/2002

such effects on the activity of an integral membrane protein. To date, several hypothesis has been entertained. These include (i) indirect effects of lipids through the alteration of properties of the bilayer, such as the fluidity (an "optimal fluidity" hypothesis; *12*, *16*) or the membrane curvature and lateral pressure (*17*, *18*), or (ii) direct effects through binding of lipids to defined sites on the transmembrane portion of the protein (*15*, *16*, *19*−*26*). The latter has led to postulate a possible role of specific lipids as peculiar "allosteric" ligands of the protein.

In this paper, we have reconstituted purified AcChR from *Torpedo* into complex lipid vesicles containing cholesterol and different phospholipid mixtures. Fourier transform infrared spectroscopy (FTIR), differential scanning calorimetry (DSC), and fluorescence anisotropy studies have been carried out in an attempt to contribute information on how the phospholipids organize in the different reconstituted bilayers. We found that under conditions reportedly required to preserve reconstituted AcChR function, i.e., presence of PA and cholesterol, a protein-induced segregation of a PA-rich membrane domain is produced. Such phenomenon seems specific for PA, as it could not be observed with any other of the phospholipids used in this work under otherwise identical experimental conditions. Fluorescence resonance energy transfer (FRET) between the receptor protein and fluorescence membrane probes shows that the PA-rich domain includes the AcChR protein.

MATERIALS AND METHODS

Cholesterol, sodium cholate, CHAPS, and crude phospholipid-rich extracts from soybean (type 2-S, asolectin lipids) were purchased from Sigma. Phosphatidylcholine from egg yolk (egg PC), dimyristoyl phosphatidylcholine (DMPC), dimyristoyl phosphatidic acid (DMPA), dimyristoyl phosphatidylserine (DMPS), dimyristoyl phsophatidylglycerol (DMPG), perdeuterated dimyristoyl phosphatidylcholine (d-DMPC), and perdeuterated dimyristoyl phosphatidic acid (d-DMPA) were purchased from Avanti Polar Lipids. [^{125}I]-α-Bungarotoxin was from New England Nuclear. The fluorophores 1,6-diphenyl-1,3,5-hexatriene (DPH) and *trans*-parinaric acid (*t*-PnA) were from Molecular Probes.

Acetylcholine Receptor Purification and Reconstitution. AcChR-enriched membranes were prepared from the electroplax of *Torpedo marmorata* (*15*, *22*). The AcChR was purified from cholate extracts of those membranes by affinity chromatography in the presence of whole asolectin lipids (*4*), followed by a last wash using egg PC (at 1 mg/mL in 1% cholate buffer) to eliminate fluorescent impurities present in asolectin. The purified AcChR eluted from the column at 1−1.5 mg of protein/mL and had specific activities of approximately 8 nmol of α-Bungarotoxin bound per mg of protein.

A detergent dialysis procedure (*15*, *22*) was used to prepare plain lipid vesicles (at ∼10 mg of phospholipids/mL) from lipid mixtures containing 25 mol % of cholesterol, 50 mol % of egg PC, and 25 mol % of either one of the phospholipids mentioned above (DMPC, DMPA, DMPG, DMPS, d-DMPC, or d-DMPA). The resulting lipid vesicles were resolubilized in 3% sodium cholate and used immediately for reconstitution of the AcChR, as described below.

Reconstituted AcChR samples were prepared from mixtures containing aliquots of purified AcChR and the solubilized lipid vesicles from above. The volume of such aliquots were chosen to yield the desired protein to phospholipid molar ratios (usually, 1:3500 or 1:560). Final concentrations in the reconstitution mixtures at high (1:560) protein-to-phospholipid ratio were AcChR, 0.8 mg/mL, and total phospholipids, 2.2 mg/mL, in buffer containing 1.3% sodium cholate. For the samples at low (1:3500) protein-to-phospholipid ratio, such concentrations were AcChR, 0.5 mg/mL, and total phospholipids, 5 mg/mL, in buffer containing 2% sodium cholate. In both cases, cholesterol was present at 25% (by mole) with respect to the phospholipids. Also, the cholate to phospholipid molar ratio was always well below 20 in order to prevent detergent damage to the AcChR protein. Reconstitution mixtures were also prepared in the absence of protein by replacing the aliquot of the purified AcChR solution by one of plain buffer of identical composition. Reconstituted vesicles were formed by dialysis at 4 °C for about 72 h (6 × 2 L changes in 10 mM Tris, pH 7.4, containing 100 mM NaCl, occasionally followed by 2 × 1 L changes in 10 mM Hepes, pH 7.4, 100 mM Na NO_3). For all the different phospholipid mixtures tested, the above dialysis procedure results in the formation of sealed unilamelar reconstituted vesicles (*4*). The vesicles were centrifuged, resuspended at suitable concentrations (see Figure legends), and stored in liquid nitrogen. Protein, phospholipid (lipid phosphorus), and cholesterol concentrations were determined as previously described (*22*). Experimentally determined protein-to-phospholipid molar ratios in samples reconstituted at nominally 1:3500 or 1:560 values ranged from 1:3500 to 1:3800 and from 1:550 to 1:700, respectively.

Infrared Measurements. The samples for FT-IR analysis were concentrated by centrifugation, resuspended into the appropriate buffer at the desired concentration (usually at 150−200 mg of phospholipids/mL), and placed (∼20−25 μL) into a liquid demountable cell (Harrick, Ossining, N. Y.) equipped with either ZnS (detection of infrared bands below 1100 cm^{-1}) or CaF_2 windows and 50 μm-thick Mylar spacers. The sample chamber was continuously purged with dry and CO_2-free air. Temperature was controlled at the desired values using a circulating water bath. FT-IR spectra were taken in a Nicolet 520 instrument equipped with a DTGS detector (*22*), at temperatures ranging 20−70 °C during a heating cycle lasting approximately 3.5 h, in which the temperature was increased by approximately 5 °C steps every 13 min, including thermal stabilization of the sample and spectral acquisition.

Differential Scanning Calorimetry (DSC). DSC was performed on a Microcal MC-2 microcalorimeter, as described previously (*27*). The difference in the heat capacities between 1.3 mL aliquots of reconstituted vesicles at the desired concentration (see Figure legends), contained in the "sample" cell of the instrument, and buffer alone in the "reference" cell was recorded by raising the temperature at a constant rate of 45 °C/h. Reported transition temperatures are those at which there is a maximum differential heat capacity, as observed in the original thermograms without any baseline corrections.

Fluorescence Anisotropy Measurements. A few microliters from stock solutions of the fluorescence probes *t*-PnA or DPH in ethanol or dimethylformamide, respectively, were

added to the reconstituted vesicle samples and allowed to stabilize for several minutes before fluorescence measurements. The ethanol or dimethylformamide final concentration in the vesicle suspension was always less than 2%. Since *t*-PnA is air-sensitive, the samples were burbled with argon and immediately sealed. In all cases, the lipid-to-probe ratio was 100 in molar terms for the anisotropy experiments.

Fluorescence spectra and steady-state anisotropy, $\langle r \rangle$, were recorded in an SLM-8000C spectrofluorimeter. Steady-state anisotropy $\langle r \rangle$, as defined by Lackowicz (*28*):

$$\langle r \rangle = (I_{VV} - G^*I_{VH})/(I_{VV} + 2^*G^*I_{VH})$$

was obtained by measuring the vertical and horizontal components of the fluorescence emission with excitation polarized vertically. The *G* factor ($G = I_{HV}/I_{HH}$) corrects for the transmissivity bias introduced by the detection system. These measurements were made with Glan-Thompson polarizers, and background intensities due to the lipid vesicles were always subtracted. In vesicle suspensions, the turbidity of the sample may severely influence the recorded anisotropy. Thus, a turbidity correction was introduced, when necessary, by extrapolation to zero concentration in a plot of anisotropy versus the apparent absorbance of the sample at the probe excitation wavelength (*29*). Excitation wavelengths for tryptophan, *t*-PnA and DPH were 280, 320, and 360 nm. respectively, and the emission was monitored at 330, 420, and 430 nm, respectively. Temperature was controlled using a circulating water bath and increased manually in the 20−50 °C range used in these studies.

Fluorescence Resonance Energy Transfer (FRET) Measurements. For the determination of the efficiency of energy transfer, aliquots of *t*-PnA (in ethanol) or DPH (in dimethylformamide) were added to a cuvette containing the reconstituted vesicles, and the quenching of tryptophan fluorescence emission at 330 nm was monitored upon excitation at 280 nm. The effect of acceptor absorption at the donor (tryptophan) excitation wavelength (280 nm.) and the acceptor absorption at donor emission wavelength (330 nm), trivial process of reabsorption were corrected as in ref *30*.

The critical radius of transfer, R_o, was calculated according to Förster (*31*):

$$R_0^{\,6} = \frac{9000(\ln 10)\kappa^2\Phi_D J}{128\pi^5 n^4 N_{AV}}$$

where Φ_D is the donor quantum yield in the absence of acceptor, *n* is the index of refraction of the medium, N_{AV} is Avogadro's number, κ^2 is the orientation factor, and *J* the overlap integral, which measures the degree of overlap between the donor emission spectrum and the acceptor absorption spectrum. A value of 1.33 was used for the refraction index of the medium (*32*), $^2/_3$ for κ^2 (*32*), and 0.29 for the tryptophan quantum yield (*33*). Absorption spectra were taken in a Beckman DU 640 spectrophotometer.

To obtain the theoretical expectation for the efficiency of energy transfer in a two-dimensional system, the approach of Gutiérrez-Merino and co-workers (*34*−*36*) was used. This theoretical model was developed to study AcChR membranes and, therefore, takes into account several specific features of this system. The plane of acceptors was simulated assuming an average area per phospholipid molecule of 0.7 nm^2 (*37*), 0.38 nm^2 per cholesterol molecule (*38*), and 0.283 nm^2 for the fluorescent probes (*39*). Moreover, this model takes into account three parameters, namely, H, which is the height of the plane of AcChR tryptophan residues respect to the plane of acceptors, *r*, the minimal distance between donor and acceptor molecules, and K_r, the apparent dissociation constant of the acceptor probe for the a putative lipid belt region (the lipid layer nearest to the protein). This last parameter provides a measure of acceptor distribution around the AcChR membrane, being random if it is 1, or nonrandom for a value distinct of 1. In this latter case, a $K_r < 1$ implies preferential location of the acceptor near the protein, and the opposite for $K_r > 1$.

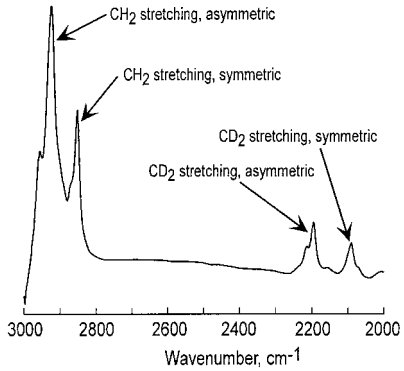

FIGURE 1: Infrared spectrum (3000−2000 cm^{-1} region) at room temperature of a reconstituted vesicle made from a 50% egg PC, 25% cholesterol, and 25% d-DMPA (by mole) lipid mixture, suspended in 10 mM Tris buffer, pH 7.4, 100 mM NaCl. Arrows within the figure indicates the position of different stretching vibrations arising from C−H and C−D bonds. CaF_2 windows were used in the spectrometer cell.

RESULTS

FTIR studies of lipid organization in the reconstituted vesicles. In natural membranes or in complex artificial reconstituted systems such as those used here, the observation of infrared bands arising from specific lipids is hampered by those from bulk lipids. To circumvent this limitation, we have made use of specific deuterated lipids as probes, in which the vibrational frequencies of the C−D bonds are markedly shifted from those of C−H bonds in the bulk lipid population (Figure 1) and, therefore, can be monitored separately (*40*−*43*). To this end, we prepared samples of AcChR reconstituted at approximately 1:3500 protein to phospholipid molar ratio, in lipid mixtures containing 50% egg PC, 25% cholesterol, and 25% of either perdeuterated DMPA (d-DMPA) or perdeuterated DMPC (d-DMPC). Such dimyristoyl derivatives were chosen as probes for these studies because of their convenient gel to liquid crystal phase transition temperatures (*44*). Figure 2 shows the changes with increasing temperature in the frequency of the CD_2 symmetric stretching band in the two reconstituted AcChR samples from above, as well as in plain lipid vesicles of identical compositions. Out of all the possible C−D vibration modes exhibited by the deuterated phospholipid probes, we selected the CD_2 symmetric stretching to illustrate our experiments because it shows the largest changes in frequency and in bandwidth with increasing temperature (*40*). Figure 2A shows that the CD_2 vibration arising from samples

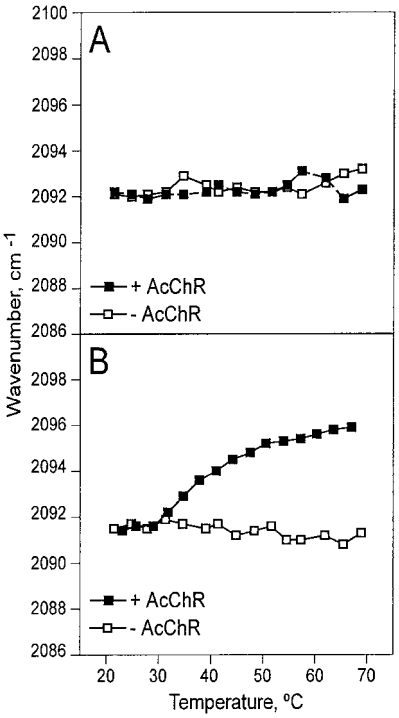

FIGURE 2: Representative temperature dependence of the infrared CD_2 symmetric stretching vibration from perdeuterated phospholipids contained in reconstituted vesicles. As indicated in the Methods section, the vesicles were prepared by detergent dialysis, in the absence (open symbols) or in the presence (filled symbols) of AcChR protein, from identical amounts of lipid mixtures containing 25 mol % of cholesterol, 50 mol % of egg PC, and 25 mol % of either d-DMPC (panel A) or d-DMPA (panel B). Protein-containing samples were prepared at a protein to phospholipid molar ratio of 1:3500, and the phospholipid concentration in the spectrometer cell was 150−200 mg/mL. All samples were in 10 mM Tris-HCl, pH 7.4, 100 mM NaCl. CaF_2 windows were used in the spectrometer cell. In these experiments as well as in those used in Figure 3, the spectra of the aqueous buffer alone at each temperature was routinely subtracted from that of the vesicle-containing sample.

containing d-DMPC does not depend on temperature and exhibits similar frequency values either in plain lipid vesicles or in the reconstituted AcChR vesicles. This suggests that mixing of the d-DMPC with the rest of the accompanying lipids, either in the absence or in the presence of AcChR protein, exhibits an ideal-like behavior. Likewise, Figure 2B shows that the CD_2 vibration arising from d-DMPA when incorporated into lipid vesicles in the absence of protein also exhibits an ideal-like behavior, similar to that found in d-DMPC samples. On the contrary, the presence of the AcChR protein in the reconstituted vesicles containing d-DMPA (Figure 2B) causes that the CD_2 vibration becomes highly temperature-dependent. This suggests that the protein induces a drastic change in the way d-DMPA is distributed within the bilayer, leading to nonideal mixing and lateral phase separation of a d-DMPA population capable to produce observable temperature-dependent spectroscopic changes. In different samples, such temperature dependence includes a frequency shift ranging 4.5−7.5 cm^{-1} and a cooperative (sigmoidal) event with an inflection point around 35−38 °C.

Monitoring the CH_2 symmetric stretching band at approximately 2854 cm^{-1}, which in these samples arises primarily from the major nondeuterated egg PC component of the vesicles, shows that in no case (i.e., regardless of the presence or the absence of d-DMPA, d-DMPC or AcChR protein) was there a temperature dependence of the CH_2 vibration (not shown). These observations suggest that the presence of the AcChR protein does not affect the temperature-dependent properties of the entire bilayer and provide further support to the occurrence of the protein-induced, d-DMPA lateral phase separation phenomena pointed out in the previous paragraph.

As an additional control, other experiments were carried out using sonicated vesicles made exclusively from pure d-DMPA at pH 6.0 and 9.0 to account for the behavior of pure monoanionic and dianionic forms of the phospholipid (not shown). The CD_2 vibration in pure DMPA samples under these conditions shifts by approximately 5 cm^{-1} and exhibits a sharp transition slightly above 50 °C and at about 45−46 °C for the monoanionic and dianionic forms, respectively. Despite the fact that the temperature scans in these experiments are taken grossly at 3−5 °C intervals, such values resemble closely the reversible gel to liquid crystal phase transition temperatures of 51 and 45 °C determined for dianionic and monoanionic forms of pure, nondeuterated DMPA (*44*).

The possibility of interconverting between monoanionic and dianionic phosphoryl forms is a unique feature of PA among all phospholipids tested in this study, and therefore, it may provide the means for specifically monitoring the polar headgroup of the PA involved in the lipid phase separation phenomenon. For this purpose, we used the same perdeuterated phospholipids-containing reconstituted samples from above (although in this case, use of deuterated or nondeuterated lipids does not provide any advantage in the monitoring of vibrations arising from the phospholipid phosphoryl group). Stretching vibrations of the dianionic and monoanionic forms of the phosphoryl group of PA have absorbance maxima at 980 and 1180 cm^{-1}, respectively (*45*, *46*). This spectral region requires ZnS windows in the IR spectrometer cell and includes contributions from other lipid components such as the choline moiety or the phosphoryl groups from other phospholipids present in the samples (*47*). Figure 3 shows the changes with temperature in the area ratio of the absorbance bands with maxima at 980 and 1180 cm^{-1}, as measured on the spectra, without deconvolution of any kind. At neutral pH and in the absence of protein, reconstituted DMPA-containing vesicles (egg PC/cholesterol/d-DMPA; 50:25:25, by mole) exhibit values for such area ratio ranging approximately 0.13−0.17. Conversely, the presence of AcChR protein in the same reconstituted lipid matrix (i.e., under conditions of lateral phase separation) causes that the area ratio decreases drastically to about 0.06, suggesting that under these conditions the protein shifts the equilibrium between the deprotonated forms of the phosphoryl group of d-DMPA, favoring the monoanionic species.

To exclude the possibility that the observed change in the area ratio comes from a contribution of the protein to the spectral region of interest, we process as a control d-DMPC-containing samples, reconstituted with and without AcChR protein, identical to those described above. Such control samples show that the presence of the protein by itself (in the absence of the PA probe) does not cause any alteration in the 980/1180 cm^{-1} area ratio (Figure 3).

Differential Scanning Calorimetry studies of lipid organization. Differential scanning calorimetry (DSC) studies

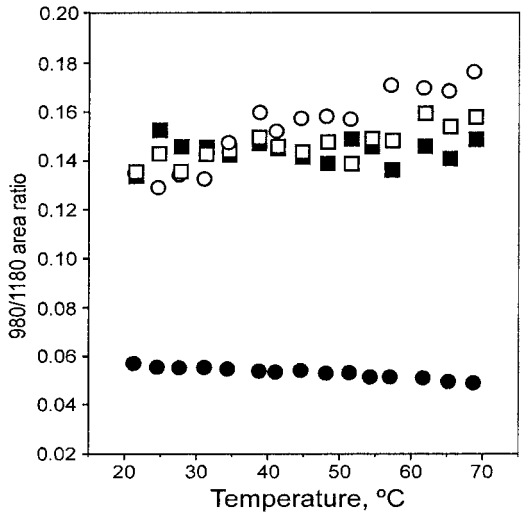

FIGURE 3: Temperature dependence of the 980 cm^{-1}/1180 cm^{-1} absorbance area ratio in the infrared spectra of reconstituted vesicles. The vesicles were prepared by detergent dialysis, in the absence (open symbols) or in the presence (filled symbols) of AcChR protein, from lipid mixtures containing 25 mol % of cholesterol, 50 mol % of egg PC and 25 mol % of either d-DMPA (circles) or d-DMPC (squares). The spectra were taken using ZnS windows in the spectrometer cell. Final concentrations of both lipids and AcChR in these samples were the same as in those used in Figure 2. All samples were in 10 mM Hepes buffer, pH 7.4, 100 mM $NaNO_3$.

have been conducted in the reconstituted vesicles in an attempt to confirm the occurrence of the protein-induced, lipid reorganization phenomena seen by FTIR. In the absence of AcChR protein, vesicles prepared from either DMPC/egg PC/Chol or DMPA/egg PC/cholesterol mixtures do not exhibit any thermal transition within the temperature range studied, as expected from complex lipid mixtures in which ideal (random) mixing of lipid components is likely to occur (Figure 4). Similarly, reconstituted vesicles made from DMPC/egg PC/Chol mixtures in the presence of AcChR protein show no transition endotherms other than that resulting from thermal denaturation of the AcChR protein (*27*, *48*). Due to the low protein concentration in these samples, the latter event produces a small and wide endotherm centered at 56−57 °C, which, because of the irreversible nature of the denaturation process, disappears completely from the thermogram in a second thermal scan of the sample (Figure 4). Additionally, samples prepared in DMPA/egg PC/cholesterol and in the presence of AcChR protein (at 1:3500 AcChR to phospholipid molar ratio, as in the FTIR samples) result in the appearance of a small and relatively narrow endotherm, with a transition temperature at approximately 41−43 °C (Figure 4). Also, an extremely wide endotherm at lower temperatures (below 35−40 °C) is seen in these samples preceding the cooperative transition observed at 41−43 °C (Figure 4). Similar to the FTIR observations on the CD_2 stretching, the above DSC experiments indicate that only when the PA probe and the AcChR protein are present simultaneously does a lipid population become reorganized in such a way as to produce observable calorimetric transitions. Comparing the FTIR and the DSC data, it is reasonable to conclude that either one or both of those endotherms is related to the temperature dependence of the infrared CD_2 vibration in the d-DMPA samples described above. Therefore, segregation (lateral phase separation) of DMPA induced by the protein appears as the obvious

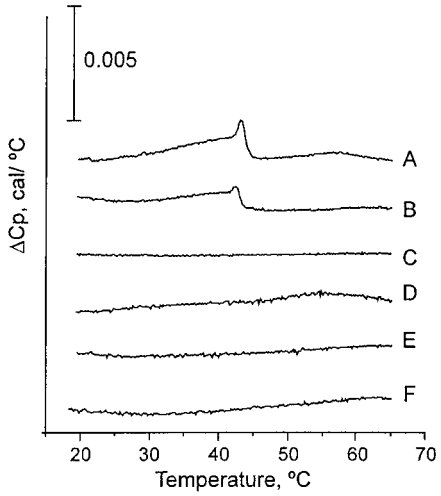

FIGURE 4: DSC studies on the effect of the AcChR protein on lipid organization in reconstituted vesicles. The thermograms shown correspond to the following: (A) reconstituted AcChR in vesicles prepared from lipid mixtures containing 25 mol % of cholesterol, 50 mol % of egg PC, and 25 mol % of DMPA; (B) second thermal scan of sample A; (C) reconstituted vesicles prepared as in sample A, but in the absence of AcChR protein; (D) reconstituted AcChR in vesicles prepared from lipid mixtures containing 25 mol % of cholesterol, 50 mol % of egg PC, and 25 mol % of DMPC; (E) second thermal scan of sample D; (F) reconstituted vesicles prepared as in sample D, but in the absence of AcChR protein. Samples containing AcChR (A, B, D, and E) were prepared at a protein to phospholipid molar ratio of 1:3500. Final concentration of either DMPC or DMPA in the calorimeter sample cell was adjusted to approximately 10 mM in all samples. The buffer used was 10 mM Tris buffer, pH 7.4, containing 100 mM NaCl.

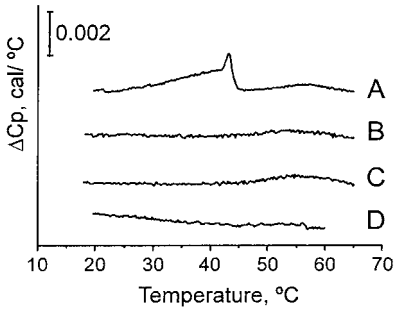

FIGURE 5: DSC studies on the effect of the AcChR protein on lipid organization in reconstituted vesicles of different composition. The thermograms shown correspond to reconstituted AcChR vesicles prepared at a protein to phospholipid molar ratio of 1:3500, from lipid mixtures containing 25 mol % of cholesterol, 50 mol % of egg PC, and either (A) 25 mol % of DMPA, (B) 25 mol % of DMPG, (C) 25 mol % of DMPC, or (D) 25 mol % of DMPS. In all cases, the final concentration of dimyristoyl phospholipids in these samples were approximately 10mM. The buffer used was 10 mM Tris, pH 7.4, 100 mM NaCl.

candidate to account for the observed calorimetric phenomena. It should also be noted that a second thermal scan of these samples still shows the above-mentioned DMPA-related endotherms, although diminished in magnitude (Figure 4).

Similar reconstituted samples were also prepared at the same protein-to-phospholipid ratios, but in the presence of other anionic phospholipid probes to further define the requirements for the lipid reorganization phenomena to take place. Figure 5 shows the DSC profiles corresponding to AcChR reconstituted samples prepared in parallel from lipid mixtures containing 50% egg PC, 25% cholesterol, and 25%

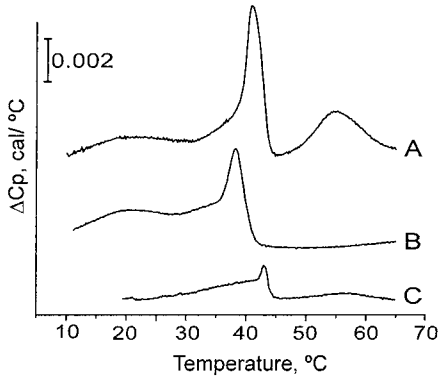

FIGURE 6: DSC studies on the effect of different AcChR/phospholipid molar ratios on lipid organization in reconstituted vesicles. The thermograms shown correspond to reconstituted AcChR vesicles prepared from lipid mixtures containing 25 mol % of cholesterol, 50 mol % of egg PC, and 25 mol % of DMPA at a protein to phospholipid molar ratio of either 1:560 (A) or 1:2500 (C). Thermogram B correspond to the second thermal scan of sample A. The concentration of DMPA in all samples was 10 mM. The buffer used was 10 mM Tris, pH 7.4, 100 mM NaCl.

of either DMPC, DMPS, DMPA, or DMPG, all having transition temperatures within the temperature range covered by the thermal scan. As shown in the figure, both the cooperative and the lower temperature endotherms indicative of lipid segregation occur exclusively in the sample containing DMPA and AcChR.

To further study the dependence of the observed DMPA segregation with the presence of the AcChR protein, reconstituted vesicles were prepared at a protein-to-phospholipid ratio higher than that used previously. Figure 6 compares the DSC thermograms obtained from samples reconstituted in parallel at protein-to-phospholipid ratios of approximately 1:3500 and 1:560. It is observed that despite of the fact that the DMPA concentrations in these samples are essentially identical (i.e., 10 mM), the DMPA-related endotherms in the sample with a higher protein concentration become much more noticeable. This suggests that at the lower protein-to-phospholipid ratios, only a fraction of the available DMPA become segregated into a membrane domain. This also means that the extent of the DMPA-related domain is limited by the amount of protein present in the reconstituted samples.

Similar to the samples reconstituted at the lower protein-to-phospholipid ratio, a second thermal scan in the high protein containing samples (Figure 6) shows that although diminished, the DMPA-related transitions still remain upon AcChR denaturation and, therefore, correspond to reversible processes. From this it follows that, although the presence of the AcChR protein is an absolute requirement for the segregation of the domain, the denatured protein partly retains the ability to maintain the DMPA domain segregated from the bulk lipid.

Fluorescence anisotropy monitoring of the AcChR-induced, DMPA segregated domain. Attempts were made to detect the presence of the DMPA domain by fluorescence anisotropy measurements because it requires a much lower amount of sample than those demanded by the FTIR or DSC procedures. For this purpose, we used mostly the *trans*-parinaric acid (*t*-PnA) and diphenylhexatriene (DPH) fluorescence probes. While *t*-PnA shows preference for partitioning into gel phases (*49*), DPH partitions evenly into gel and fluid phases, entering deeply into the lipid bilayer, aligned with the phospholipid acyl chains (*50*).

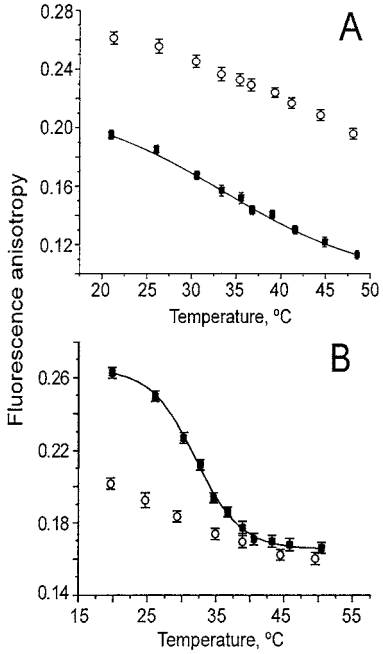

FIGURE 7: Fluorescence anisotropy studies on the effect of the AcChR protein on lipid organization in reconstituted vesicles. Anisotropy of the fluorescent probes, DPH (panel A) or *t*-PnA (panel B), was determined at different temperatures in reconstituted vesicles prepared from lipid mixtures containing 25 mol % of cholesterol, 50 mol % of egg PC, and 25 mol % of DMPA with (filled symbols) or without (open symbols) AcChR protein. When present, AcChR was at a protein-to-phospholipid molar ratio of 1:560. The DMPA concentration is 0.12 mM in all samples. The buffer used was 10 mM Tris, pH 7.4, 100 mM NaCl. Standard error bars for a representative experiment are given.

Figure 7 shows representative temperature-dependent, fluorescence anisotropy values for these two probes incorporated into AcChR reconstituted vesicles prepared at high protein-to-phospholipid ratios (1:560) from 50% egg PC: 25% cholesterol:25% DMPA mixtures. Fluorescence anisotropy data from identical plain lipid vesicles (reconstituted in the absence of protein) are also included for comparison. In the absence of protein, temperature-dependent changes in the fluorescence anisotropy of the DPH probe are essentially linear, decreasing progressively with increasing temperature (Figure 7A). The presence of AcChR protein in the reconstituted samples causes that DPH fluorescence anisotropy drops down considerably at all temperatures studied (i.e., the membrane regions explored by the DPH probe become more "fluid" in the presence of protein). Similar changes in DPH anisotropy have been reported in the incorporation of integral membrane proteins into lipid vesicles (*51*, *52*). In the latter samples, it is also observed that the dependence of the DPH fluorescence anisotropy with temperature departs slightly from being linear and tends to adopt a sigmoid shape with an inflection point at 33 ± 2 °C (Figure 7A).

Fluorescence anisotropy of the *t*-PnA probe in the protein-containing vesicles (Figure 7B) exhibits a clearly sigmoidal dependence with temperature, with a well-defined inflection point at 32 ± 3 °C, which is similar to that poorly defined from DPH anisotropy (see above). These observations suggest that both fluorescence probes are sensing the same

AcChR-induced, DMPA-related phenomena detected by FTIR or DSC methods. Also, it is observed that anisotropy values for *t*-PnA below the inflection (transition) temperature in the AcChR-containing samples are much higher than that in the absence of protein (Figure 7B). In fact, such values are near typical *t*-PnA anisotropy values of 0.28−0.30 reported for a pure gel phase (*52*, *53*), indicating that the putative AcChR-induced DMPA domain is "gel-like" and considerably ordered. Indeed, this might partly explain why *t*-PnA is a better probe for this domain than DPH: *t*-PnA is known to preferentially partition into gel phases, while DPH does not. Therefore, because the observed anisotropy is an average from the whole membrane, the *t*-PnA probe is likely to monitor more precisely events occurring within the gel-like DMPA domain, into which it preferentially partitions.

Location of the AcChR protein relative to the DMPA-rich domain. Following the rationale from above, we have used fluorescence resonance energy transfer between the protein tryptophan residues as energy donors and the DPH and *t*-PnA probes as energy acceptors, to determine whether the protein is within Förster distance from the membrane domains into which these probes partition. AcChR reconstituted at a protein-to-phospholipid ratio of 1:560, in egg PC:cholesterol:DMPA (50:25:25 by mole) and egg PC:cholesterol:DMPC (50:25:25 by mole), were used in these experiments at a temperature of 20 °C, that is, below the DMPA-rich domain transition temperature. R_o for each of the donor−acceptor pairs were calculated from the spectral overlap (not shown). Calculated R_o values were 26.8 ± 0.7 and 32.7 ± 0.2 Å for the tryptophan-*t*-PnA and tryptophan-DPH pairs, respectively. To analyze the energy transfer data, we used the Gutierrez-Merino model for two-dimensional systems (see ref *33* and references therein). In this model, specifically developed for AcChR membranes, changes in transfer efficiency with acceptor surface density depend on three variables: H, the distance between the plane containing the donor and that of the acceptor, normal to the membrane; *r*, the distance of closest approximation between the donor and the acceptor; and K_r, the apparent dissociation constant for a putative lipid domain surrounding the AcChR protein (*33*). Obviously, to calculate one of the above three variables, the other two must either be known or fixed to presumed values. Tryptophan residues in the transmembrane portion of the AcChR are proposed to form a coplanar ring lying parallel to the membrane surface, approximately 10 Å deep (*54*). On the basis of such report, we arbitrarily fixed $H = 10$ Å for the analysis of the tryptophan−DPH transfer data. Also, since DPH does not show any preference for partitioning into gel or fluid phases, we assumed $K_r = 1$, which according to the Gutierrez-Merino model corresponds to a random distribution of the fluorophore within the membrane (*33*). Under these assumptions, the best fit of the experimental data from the tryptophan−DPH transfer to the Gutierrez-Merino model is that corresponding to $r = 30$ Å (Figure 8A). This value of $r = 30$ Å was then used, along with the same value of $H = 10$ Å, to calculate K_r for the *t*-PnA probe. Energy transfer data for the egg PC:cholesterol:DMPA reconstituted membranes (Figure 8B) show that the best fit corresponds to $K_r = 0.6 \pm 0.1$. On the other hand, in the egg PC:cholesterol:DMPC, in which there is no domain segregation (negative control), the best value corresponds to $K_r = 1 \pm 0.1$ (Figure 8C). As discussed extensively in Antollini et al. (*33*), values

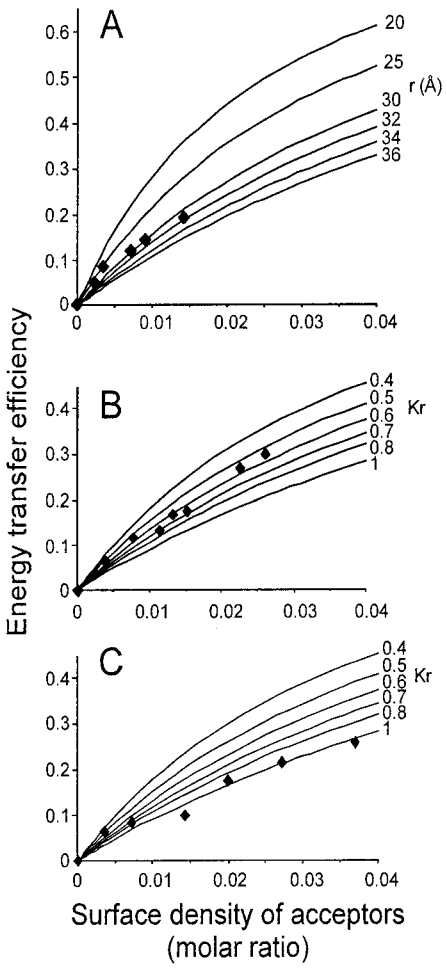

FIGURE 8: Efficiency of fluorescence energy transfer from tryptophan as the energy donor, as a function of the surface density of acceptors in reconstituted AcChR vesicles. Panel A shows representative results obtained using DPH as the energy acceptor in reconstituted AcChR vesicles made from egg PC−cholesterol−DMPA lipid mixtures. Theoretical curves (continuous lines) in this panel correspond to predictions from the Gutierrez-Merino model (*33*) for different values of *r*, the donor−acceptor minimal distance, and fixed values of $H = 10$ Å and $K_r = 1$. Panels B and C correspond to results obtained using *t*-PnA as the energy acceptor in reconstituted AcChR vesicles prepared from either egg PC−cholesterol−DMPA (panel B) or egg PC−cholesterol−DMPC (panel C) lipid mixtures. Theoretical curves (continuous lines) in panel B and C represent the predictions from the Gutierrez-Merino model for different values of K_r, the apparent dissociation constant of *t*-PnA for a putative lipid domain surrounding the AcChR protein, and fixed values of $r = 30$ Å and $H = 10$ Å. The protein to phospholipid molar ratio in the reconstituted vesicles was kept constant at 1:560, and the samples were in 10 mM Tris buffer, pH 7.4, 100 mM NaCl. The temperature was 20 °C.

of K_r lower that 1 indicate a preferential location of the *t*-PnA probe in membrane regions immediately surrounding the protein, within Förster distance of the tryptophan donors, while a K_r value of 1 indicates random distribution. These results provide additional support to the existence of a gel-like, DMPA-rich membrane domain induced by the AcChR, but more importantly, they strongly suggest that the protein itself is included in such domain.

DISCUSSION

This study provides direct evidence that reconstitution of purified AcChR protein into complex lipid membranes

containing PA, directs the segregation of a PA-rich membrane domain even at low protein-to-lipid ratios. The data to support such conclusion come from using specific phospholipid probes (dimyristoyl phospholipids) in three different techniques (FT-IR, DSC, and fluorescence anisotropy) which qualitatively confirm it, but also provide unique information on the specific features of the domain. Thus, monitoring of the CD_2 vibration from individual perdeuterated phospholipids by FT-IR serves to unequivocally identify the involvement of the DMPA probe in the protein-induced lateral phase separation phenomena (Figure 2), while changes in the anisotropy of the fluorescent *t*-Pna probe, going from gel-like to liquid crystal values with increasing temperature, suggest that the observed DMPA-related, temperature-dependent event represents a cooperative transition from a highly ordered to a disordered phase (Figure 7). Nevertheless, transition temperatures determined for the DMPA-rich domain by the different techniques differ significantly. In this regard, it should be noted that the different techniques rely on different physical principles (including the addition of an extrinsic probe, as in the case of fluorescence) and are used at different heating rates, using samples prepared at different protein-to-phospholipid ratios. In our interpretation, such differences in experimental conditions should account for most of the variability observed in determining the domain's transition temperature.

The application of the Gutierrez-Merino model to the FRET data indicates that the AcChR protein is included in the domain, within Förster distance of the gel-like lipid phase explored by the *t*-Pna fluorescence probe (Figure 8; see ref *33* for an extensive discussion on this model). Therefore, the domain could be envisioned as formed by units in which the AcChR molecules are surrounded by ordered shells of DMPA molecules, sequestered from the bulk lipid by interaction with the protein. This seems consistent with the observation that phosphatidic acid has one of the highest affinities of all lipid classes for binding to the AcChR protein (*20*, *55*−*58*). Moreover, because the domain exhibits a certain degree of cooperativity to undergo the phase transition, the AcChR-lipid shell units or "microdomains" would be expected to coalesce into larger domains in order to provide a macroscopically observable behavior. An estimation of the minimal size for the segregated DMPA domain can in principle be obtained from the heat involved in the observed DSC thermal events, according to the expression

$$n_{\mathrm{DMPA}} = Q/\Delta H_{\mathrm{DMPA(domain)}}$$

Where n_{DMPA} represents the number of moles of DMPA undergoing the observed transition, Q, the heat involved, and $\Delta H_{\mathrm{DMPA(domain)}}$ the apparent molar transition enthalpy of DMPA in the domain. Despite difficulties to define a baseline, Q, the heat involved in the observed transitions could be grossly estimated from the thermograms. As to the $\Delta H_{\mathrm{DMPA(domain)}}$, we have no way to know its value, and instead, we assumed that the molar transition enthalpy for DMPA in the domain is as high as that of the pure phospholipid (3.82 kcal/mol in this type of reconstituted, large unilamellar vesicles) as the least favorable hypothesis. This should underestimate n_{DMPA}, the number of moles of DMPA undergoing the calorimetric transitions. Nevertheless, our estimates indicate that about 220 and 120 mol of DMPA were segregated per mol of AcChR protein, respectively, in samples prepared at low (1:2500) and high (1:560) protein to phospholipid molar ratios. Moreover, because *Torpedo* AcChR exists primarily as a dimer linked by a disulfide bond between adjacent δ subunits, which is preserved in our preparations (*4*), the AcChR/lipid shell units referred above would be formed by AcChR dimers, each surrounded by approximately 240−440 DMPA molecules. These estimates exceed by far the reported capacity of the transmembrane region of the AcChR protein to bind phospholipids (∼45 phospholipid binding sites per AcChR monomer, *13*, and therefore, our observations cannot be understood solely in terms of a pure hydrophobic lipid−protein interaction. Furthermore, DSC data also show that the segregated domain is heterogeneous and gives raise to at least two different endotherms corresponding to lipid transitions with different cooperativity (Figures 4 and 6). A possible explanation for both the heterogeneity and the large number of interacting lipids is that, in addition to hydrophobic lipid−protein interactions, hydrophilic interactions between the DMPA polar headgroup and the bulky, mushroom-shaped extracellular portion of the protein could contribute to maintain the segregated domain. A somewhat similar phenomenon has been reported for the erythrocyte membrane protein glycophorin (*59*). In any case, whatever the interactions might be, the results shown in Figures 4 and 6 on the second thermal scans in these samples indicate that the protein determinants involved in maintaining the segregated domain are mostly retained upon thermal denaturation.

As mentioned above, such microdomains would have to coalesce to be able to exhibit observable macroscopic properties, and then, it would be expected that the resulting larger DMPA domain would exhibit phase transition features similar to that of the pure phospholipid. This, however, is not the case, and the transition temperature for the DMPA domain, as determined by the different techniques used in this work, is much lower than expected for a pure DMPA transition. Other features of the phase transition of the DMPA-rich domain, such as a lower cooperativity or a larger frequency shift compared to a pure DMPA phase transition, are also observed. Besides possible perturbations coming from the presence of the protein itself (which are likely to occur), an additional reason for this unexpected behavior could be that the segregated domain includes other lipids in addition to DMPA. In principle, cholesterol appears as a likely candidate to enter into the domain because it also has a relatively high affinity for binding to cholesterol sites on the receptor protein (*20*, *25*). In such a case, since cholesterol decreases greatly the apparent molar enthalpy of the DMPA phase transition in DMPA:cholesterol vesicles (not shown), our estimates on the number of phospholipids segregated per AcChR molecule should be corrected to include an even larger number of DMPA molecules.

Several questions remain as to defining (i) why there is selectivity for PA in the AcChR-induced segregation of the domain and (ii) how domain formation overcomes the entropically favorable mixing of lipid components in the membrane. In the former, it has been reported that PA and cholesterol, the most effective lipids in preserving reconstituted AcChR function, are among those that bind to the protein with a higher affinity (*20*, *55*−*58*). This suggests that lipid binding to the protein should be an important factor in

initiating domain formation. Denisov et al. (*60*) have reported that binding of basic peptides to membranes produces the formation of lateral domains enriched in acidic phospholipids. Those authors explained their results on the basis of electrostatic interactions by which the decrease in the membrane net charge density accompanying binding of acidic phospholipids to the basic peptides decreases sufficiently the electrostatic free energy as to overcome the free energy of mixing of neutral and acidic phospholipids, thus resulting in a net decrease in the overall free energy of the system to favor domain formation. In this regard, photolabeling studies aimed to identify lipid exposed regions of the AcChR (*21*, *23*) concluded that a stretch of the α-subunit polypeptide chain containing the proposed transmembrane segment M4 becomes efficiently labeled by a photoactivatable derivative of phosphatidylserine (*21*). Such M4 membrane spanning region is flanked by two positively charged amino acids, Arg-429 and His-408, which, according to models of transmembrane organization of AcChR subunits (*61*), are located at the level of the phospholipid headgroups, near the membrane surface. Similar findings regarding the presence of positively charged residues at the end of the M1, M3, and M4 lipid-exposed, membrane-spanning regions in different AcChR subunits have also been reported (*62*). In principle, such positively charged residues could provide suitable interaction sites for the negatively charged headgroups of acidic phospholipids, in a manner similar to that of the basic peptides studied by Denisov et al. (*60*). Nevertheless, salt screening and pH titration experiments using spin-labeled phospholipid analogues have concluded that in the AcChR (*63*), as well as in other large integral membrane proteins (*64*, *65*), electrostatic interactions do not suffice to account for the selectivity exhibited for binding of acidic phospholipids. Our own data emphasize that other classes of anionic phospholipids cannot substitute the PA derivative in domain segregation, despite having the same charge at neutral pH and an identical fatty acid composition. This lead us to conclude that rather than electrostatic interactions alone, the observed selectivity must be determined by subtle molecular details of the interaction between the entire phospholipid headgroup and specific sites in the AcChR protein. In any case, sorting of additional lipid molecules ("propagation") to form the observed larger domains must follow the initial phospholipid binding to the protein. In such a process, it seems reasonable to assume that electrostatic contributions would be most important. Indeed, the shift in the equilibrium between the deprotonated forms of the phosphoryl group of DMPA in the segregated domain favoring the monoanionic species (Figure 3) seems consistent with decreasing sufficiently the electrostatic contribution to the free energy of the system (*60*) to favor the formation of membrane domains enriched in the monoanionic phospholipid.

Recently, a FT-IR study using AcChR reconstituted at 1:150 protein to phospholipid molar ratio in 3:2 1-palmitoyl-2-oleoyl phosphatidylcholine/perdeuterated 1-palmitoyl-2-oleoyl phosphatidic acid as the lipid matrix (*66*) reported clear effects on bilayer properties as a consequence of PA-AcChR interactions. However, at variance with our conclusion on the segregation of the DMPA-rich domain, such report argued against the occurrence of phase separation of zwitterionic and anionic phospholipids in the presence of AcChR. A possible explanation for this apparent discrepancy could be that, at the much higher protein-to-phospholipid ratio used by those authors, in which the number of PA molecules barely exceeds the number of phospholipid binding sites on the AcChR (∼45 phospholipid binding sites per AcChR monomer, *13*), the detection of the expected transition of the deuterated PA is prevented because most PA molecules are strongly protein bound. Nonetheless, despite the apparent discrepancy, it seems likely that the PA−AcChR interactions detected by those authors (*66*) could also be those that under the appropriate experimental conditions, lead to the domain segregation phenomena reported here.

How relevant could the above findings be to natural membranes? Our observations on the selectivity for PA seen both, in its interaction with the AcChR protein and in domain formation seem reminiscent of those reported for envelope proteins of vesicular stomatitis virus (*67*). Despite the low concentration of PA in natural membranes, the viral proteins interact specifically with PA and form PA-enriched domains in the host membrane, which are essential for budding of new viral particles. From the observations reported here, it is obvious that the reconstituted AcChR, even at very low protein-to-lipid ratios, also sequesters quite efficiently and specifically a large number of PA molecules by sorting them out from complex lipid mixtures. In *Torpedo* membranes the concentration of PA is also low, but it increases by 2−3-fold in membrane fractions having a higher AcChR content (*68*). Therefore, it seems conceivable that the AcChR in the native *Torpedo* membranes, with protein-to-lipid ratios comparable to the highest used here (*68*, *69*), could sequester PA from its surroundings and configures a PA-rich microdomain, as large as the availability of such phospholipid permits. Considering that PA has long been known to be required to preserve reconstituted AcChR function, the possibility that such a regulatory role could be mediated by the segregation of a PA-rich membrane domain introduces a new conceptual element in this field that might also be relevant for other membrane proteins. As to other types of nicotinic AcChR's, it has been reported that a "raft"-like domain containing at least cholesterol and GM1 ganglioside is involved in clustering neuronal α7 AcChR in the areas of synaptic contact (*70*). In any case, the above ideas on lipid−AcChR interactions should also take into account the dynamics of the process. Studies based on spin-labeled probes postulated that, because the exchange between protein-bound and protein-free lipids is expected to be rather fast (*56*, *71*), an important factor in determining the effects of lipids on the protein is the time-averaged composition of the protein-bound lipid population. In this regard, domain formation should dramatically increase the probability of exposure of the protein to the domain components, obviating the fact that certain lipids might be present in natural membranes at low concentration.

ACKNOWLEDGMENT

We thank our colleagues Dr. A. Ferrer-Montiel and Dr. J. Gómez for their critical reading of the manuscript. We also thank Mr. Pascual and Joaquin Sempere for providing the live *Torpedo marmorata* and the "Ayuntamiento de Santa Pola" for the use of their aquarium facilities.

REFERENCES

1. Barnard, E. A. (1992) *Trends. Biochem. Sci. 17*, 368−374.
2. Ortells, M. O., and Lunt, G. G. (1995) *Trends. Neurosci. 18*, 121−127.
3. Corringer, P. J., Le Novere, N., and Changeux, J. P. (2000) *Annu. Rev. Pharmacol. Toxicol. 40*, 431−458.
4. McNamee, M. G., Jones, O. T., and Fong, T. M. (1986) in *Ion Channel Reconstitution* (Miller, C., Ed.) pp 231−273, Plenum Press, New York.
5. Galzi, J. L., and Changeux, J. P. (1995) *Neuropharmacology 34*, 563−582.
6. Hucho, F., Tsetlin, V. I., and Machold, J. (1996) *Eur. J. Biochem. 239*, 539−557.
7. Sine, S. M. (1993) *Proc. Natl. Acad. Sci. U.S.A. 90*, 9436−9440.
8. Ochoa, E. L., Chattopadhyay, A., and McNamee, M. G. (1989) *Cell. Mol. Neurobiol. 9*, 141−178.
9. Bouzat, C., and Barrantes, F. J. (1997) *Mol. Membr. Biol. 14*, 167−177.
10. Miyazawa, A., Fujiyoshi, Y., Stowell, M., and Unwin, N. (1999) *J. Mol. Biol. 288*, 765−786.
11. Criado, M., Eibl, H., and Barrantes, F. J. (1984) *J. Biol. Chem. 259*, 9188−9198.
12. Fong, T. M., and McNamee, M. G. (1986) *Biochemistry 25*, 830−840.
13. Jones, O. T., Eubanks, J. H., Earnest, J. P., and McNamee, M. G. (1988) *Biochemistry 27*, 3733−3742.
14. Sunshine, C., and McNamee, M. G. (1992) *Biochim. Biophys. Acta 1108*, 240−246.
15. Fernández, A. M., Fernández-Ballester, G., Ferragut, J. A., and González-Ros, J. M. (1993) *Biochim. Biophys. Acta 1149*, 135−144.
16. Baenziger, J. E., Morris, M. L., Darsaut, T. E., and Ryan, S. E. (2000) *J. Biol. Chem. 275*, 777−784.
17. Cantor, R. S. (1997) *J. Phys. Chem. 101*, 1323−1325.
18. de Kruijff, B. (1997) *Nature 386*, 129−130.
19. Fong, T. M., and McNamee, M. G. (1987) *Biochemistry 26*, 3871−3880.
20. Jones, O. T., and McNamee, M. G. (1988) *Biochemistry 27*, 2364−2374.
21. Blanton, M. P., and Wang, H. H. (1990) *Biochemistry 29*, 1186−1194.
22. Fernández-Ballester, G., Castresana, J., Fernández, A. M., Arrondo, J. L. Ferragut, J. A., and González-Ros, J. M. (1994) *Biochem. Soc. Trans. 22*, 776−780.
23. Corbin, J., Wang, H. H., and Blanton, M. P. (1998) *Biochim. Biophys. Acta 1414*, 65−74.
24. Addona, G. H., Sandermann, H., Jr, Kloczewiak, M. A., Husain, S. S., and Miller, K. W. (1998) *Biochim. Biophys. Acta 13*, 299−309.
25. Santiago, J., Guzmán, G. R., Rojas, L. V., Marti, R., Asmar-Rovira, G. A., Santana, L. F., McNamee, M., and Lasalde-Dominicci, J. A. (2001) *J. Biol. Chem. 276*, 46523−46532.
26. Fernandez-Ballester, G., Castresana, J., Fernández, A. M., Arrondo, J. L., Ferragut, J. A., and Gonzalez-Ros, J. M. (1994) *Biochemistry 33*, 4065−4071.
27. Artigues, A., Villar, M. T., Ferragut, J. A., and Gonzalez-Ros, J. M. (1987) *Arch. Biochem. Biophys. 258*, 33−41.
28. Lackowicz, J. R. (1983) in *Principles of Fluorescence Spectroscopy*, Plenum Press, NewYork.
29. Mateo, C. R., Lillo, M. P., Gonzalez-Rodriguez, J., and Acuña, A. U. (1991) *Eur. Biophys. J. 20*, 41−52.
30. Coutinho, A., and Prieto, M. (1993) *J. Chem. Ed. 70*, 425.
31. Förster, T. (1959) *A. Naturforsch. A. Astrophys. Phys. Chem. 4*, 321.
32. Valenzuela, C. F., Weign, P., Yguerabide, J., and Jonson, D. A. (1994) *Biophys. J. 66*, 674−682.
33. Antollini, S. S., Soto, M. A., Bonini de Romanelli, I., Gutierrez-Merino, C., Sotomayor, P., and Barrantes, F. J. (1996) *Biophys. J. 70*, 1275−1284.
34. Gutierrez-Merino, C., Munkonge, F., Mata, A. M., East, J. M., Levinson, B. L., Napier, R. M., and Lee, A. G. (1987) *Biochim. Biophys. Acta 897*, 207−216.
35. Gutierrez-Merino, C., Centeno, F., Garcia-Martin, E., and Merino, J. M. (1994) *Biochem. Soc. Trans. 22*, 784−788.
36. Gutierrez-Merino, C., Bonini de Romanelli, I. C., Pietrasanta, L. I., Barrantes, F. J. (1995) *Biochemistry 34*, 4846−4855.
37. Thomas, D. D., Caslsen, W. F., and Stryer, L. (1978) *Proc. Natl. Acad. Sci. U.S.A. 75*, 5746−5750.
38. Ipsen, J. H., Mouritsen, O. G., and Bloom, M. (1990) *Biophys. J. 57*, 405−412.
39. Mateo, C. R., Lillo, M. P., Brochon, J. C., Martínez-Ripoll, M., Sanz-Aparicio, J., and Acuña, A. U. (1993) *J. Phys. Chem. 97*, 3486−3491.
40. Casal, H. L., and Mantsch, H. H. (1984) *Biochim. Biophys. Acta 779*, 381−401.
41. Jaworsky, M., and Mendelsohn, R. (1986) *Biochim. Biophys. Acta 860*, 491−502.
42. Mantsch, H. H., and McElhaney, R. N. (1991) *Chem. Phys. Lipids 57*, 213−226.
43. Arrondo, J. L., and Goni, F. M. (1998) *Chem. Phys. Lipids 96*, 53−68.
44. Blume, A. (1988) in *Physical Properties of Biological Membranes and Their Functional Implications* (C. Hidalgo, Ed.) pp 71−121, Plenum Press, New York.
45. Sanchez-Ruiz, J. M., and Martinez-Carrion, M. (1988) *Biochemistry 27*, 3338−3342.
46. Bhushan, A., and McNamee, M. G. (1993) *Biophys. J. 64*, 716−723.
47. Tamm, L. K., and Tatulian, S. A. (1993) *Biochemistry 32*, 7720−7726.
48. Castresana, J., Fernández-Ballester, G., Fernández, A. M., Laynez, J. L., Arrondo, J. L., Ferragut, J. A., and Gonzalez-Ros, J. M. (1992) *FEBS Lett. 314*, 171−175.
49. Sklar, L. A., Miljanich, G. P., and Dratz, E. A. (1979) *Biochemistry 18*, 1707−1716.
50. Lentz, B. R., Barenholz, Y., and Thompson, T. E. (1976) *Biochemistry 15*, 4529−4537.
51. Sunshine, C., and McNamee, M. G. (1994) *Biochim. Biophys. Acta 1191*, 59−64.
52. Dergunov, A. D., Taveirne, J., Vanloo, B., Caster, H., and Rosseneu, M. (1997) *Biochim. Biophys. Acta 1346*, 131−146.
53. Ben-Yashar, V., and Barenholz, Y. (1989) *Biochim. Biophys. Acta 985*, 271−278.
54. Chattopadhyay, A., and McNamee, M. G. (1991) *Biochemistry 30*, 7159−7164.
55. Marsh, D., and Barrantes, F. J. (1978) *Proc. Natl. Acad. Sci. U.S.A. 75*, 4329−4333.
56. Ellena, J. F., Blazing, M. A., and McNamee, M. G. (1983) *Biochemistry 22*, 5523−5535.
57. Esmann, M., and Marsh, D. (1985) *Biochemistry 24*, 3572−3578.
58. Dreger, M., Krauss, M., Herrmann, A., and Hucho, F. (1997) *Biochemistry 36*, 839−847.
59. Ruppel, D., Kapitza, H. G., Galla, H. J., Sixl, F., and Sackmann, E. (1982) *Biochim. Biophys. Acta 692*, 1−17.
60. Denisov, G., Wanaski, S., Luan, P., Glaser, M., and McLaughlin, S. (1998) *Biophys. J. 74*, 731−744.
61. Noda, M., Takahashi, H., Tanabe, T., Toyosato, M., Kikyotani, S., Furutani, Y., Hirose, T., Takashima, H., Inayama, S., Miyata, T., and Numa, S. (1983) *Nature 302*, 528−532.
62. Blanton, M. P., and Cohen, J. B. (1992) *Biochemistry 31*, 3738−3750.
63. Raines, D. E., and Miller, K. W. (1993) *Biophys. J. 64*, 632−641.
64. Esmann, M., Watts, A., and Marsh, D. (1985) *Biochemistry 24*, 1386−1393.
65. Horvath, L. I., Brophy, P. J., and Marsh, D. (1988) *Biochemistry 27*, 5296−5304.
66. daCosta, C. J., Ogrel, A. A., McCardy, E. A., Blanton, M. P., and Baenziger, J. E. (2002) *J. Biol. Chem. 277*, 201−208.
67. Luan, P., Yang, L., and Glaser, M. (1995) *Biochemistry 34*, 9874−9883.
68. Gonzalez-Ros, J. M., Llanillo, M., Paraschos, A., and Martinez-Carrion, M. (1982) *Biochemistry 21*, 3467−3474.
69. Martinez-Carrion, M., Gonzalez-Ros, J. M., Mattingly, J. R., Ferragut, J. A., Farach, M. C., and Donnelly, D. (1984) *Biophys. J. 45*, 141−143.
70. Bruses, J. L., Chauvet, N., and Rutishauser, U. (2001) *J. Neurosci. 21*, 504−512.
71. East, J. M., Melville, D., and Lee, A. G. (1985) *Biochemistry 24*, 2615−2623.

BI0200099